Discontinuous Equilibrium Titrations of Cooperative Calcium Binding to Calmodulin Monitored by 1-D ^{1}H-Nuclear Magnetic Resonance Spectroscopy†

Susan Pedigo and Madeline A. Shea*

Department of Biochemistry, University of Iowa College of Medicine, 51 Newton Road, 4-303 BSB Iowa City, Iowa 52242-1109

Received January 23, 1995; Revised Manuscript Received May 17, 1995®

ABSTRACT: Calmodulin binds up to four calcium ions cooperatively in response to cellular signaling events. To understand the functional energetics of calcium activation of calmodulin, it is important to monitor individual Ca^{2+}-binding sites and other positions at partial degrees of saturation. This study is the first use of 1-D proton NMR to monitor the *equilibrium* Ca^{2+}-binding properties of calmodulin. Protein concentrations required for NMR experiments (~1 mM) are ~1000-fold greater than the K_d values for calcium binding to calmodulin, preventing a direct continuous equilibrium titration of calmodulin. Thus, dialysates of calmodulin in buffers of experimentally determined $[Ca^{2+}]_{free}$ were prepared to conduct *discontinuous equilibrium* titrations at both 92 and 152 mM KCl. For the C-terminal domain, the normalized area of the δ-protons of Y138 defined calcium binding isotherms. For N-terminal domain resonances ($F16_{C\delta H}$, $T26_{C\alpha H}$, $D64_{C\alpha H}$, and $F65_{C\delta H}$), the calcium-dependent change in chemical shift defined isotherms. These are the first residue-specific studies to monitor the energetics of Ca^{2+} binding to the N-terminal domain in wild-type holo calmodulin. Calcium binding to both domains appeared cooperative and binding affinity decreased in higher KCl. Isotherms resolved from the side chain resonances of F16 and F65 had a lower median ligand activity and a slightly higher degree of cooperativity than isotherms resolved from the backbone resonances of D64 and T26. Salt-dependent changes in apparent intradomain cooperativity differed for the domains: at higher salt, ΔG_c increased for the C-terminal domain while remaining constant or decreasing for the N-terminal domain.

Calmodulin (CaM)[1] is a ubiquitous four-site calcium-binding protein of the EF-hand family (Kretsinger, 1976) and serves as the primary intracellular calcium receptor in most eukaryotic cells. Calcium binds to calmodulin cooperatively, activating it to regulate myriad tissue-specific cellular processes (see Cohen & Klee, 1988 and Török & Whitaker, 1994). The interplay between local binding interactions and global conformational change form the basis for the switching process triggered by calcium binding. An understanding of the molecular mechanism of this cooperativity requires determination of the number and properties of conformational states populated by calmodulin, the intrinsic free energies of calcium binding to each of the four sites, and the degree of intradomain and interdomain cooperativity. This report describes the first use of NMR to monitor *equilibrium* calcium titrations of calmodulin in an effort to deduce residue-specific binding isotherms and thereby better understand the energetic contributions of individual domains and sites within this small but complex protein.

Calmodulin has a repetitive structure configured in an $\alpha-\beta-\alpha'-\beta'$ pattern of EF-hand motifs (Figures 1 and 2; Babu *et al.*, 1988). Each domain contains two of these motifs with a short region of antiparallel β-sheet connecting each pair of calcium-saturated sites. NMR studies show that the β-sheets are maintained in co-complexes with target peptides [cf. Seeholzer and Wand (1989)] but the interaction between the α' and β' segments of apo CaM is absent under low salt conditions (Urbauer *et al.*, 1995). The structure of the linker region between domains appears to be variable and highly dependent on solution conditions (Bayley & Martin, 1992; Török *et al.*, 1992). Crystallographic and heteronuclear, multidimensional NMR studies have elucidated solution structures of calcium-saturated calmodulin both in the absence and presence of target peptides (Babu *et al.*, 1988; Meador *et al.*, 1992, 1993; Ikura *et al.*, 1992a, 1992b; see Török & Whitaker, 1994 for review). These studies demonstrated flexibility of the linker between the domains and showed that the domains are in close proximity when both are interacting with a peptide. However, studies of calcium-saturated calmodulin do not address the mechanism of calcium-induced switching from the apo to fully saturated form. To understand the structural and energetic nature of this transition, it must be studied directly.

The goal of this study is to understand the mechanism of energy transduction from local changes that are triggered by binding of calcium at each of the four sites to the resulting global conformational changes of calmodulin. However, this requires the study of intermediate (partially saturated) ligation species of macromolecules which is never straightforward. Two approaches to study these forms of calmodulin would be (1) to determine the fractional abundance of protein with

† These studies were supported by grants to M.A.S. from the American Heart Association (AHA 91014980), National Science Foundation Presidential Young Investigator Award (NSF MCB 9057157), and N.I.H. Diabetes and Endocrinology Research Center (DK 25295). S.P. was supported by an N.I.H. Predoctoral Traineeship in Biotechnology (PHS 1 T32 GM08365-04).

® Abstract published in *Advance ACS Abstracts,* August 1, 1995.

[1] Abbreviations: BAPTA, 1,2-bis(*o*-aminophenoxy)ethane-*N,N,N',N'*-tetraacetic acid; CaM, calmodulin; CD, circular dichroism; difluoro-BAPTA, 4,4'-difluoro-1,2-bis(*o*-aminophenoxy)ethane-*N,N,N',N'*-tetraacetic acid; EndoGluC, endoproteinase GluC; EGTA, ethylene glycol bis(β-aminoethyl ether)-*N,N,N',N'*-tetraacetic acid; FID, free induction decay; HEPES, *N*-(2-hydroxyethyl)piperazine-*N'*-2-ethanesulfonic acid; NTA, nitrilotriacetic acid; NMR, nuclear magnetic resonance; NOE, nuclear Overhauser effect; ppm, part per million; TSP, 3-(trimethylsilyl)propionate.

0006-2960/95/0434-10676$09.00/0

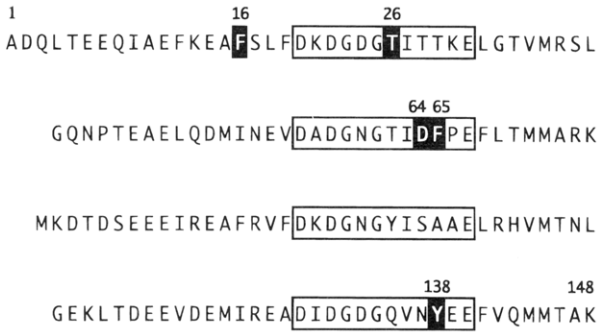

FIGURE 1: Amino acid sequence of rat and bovine calmodulin. The sequence was divided into four segments. Segment α (residues 1−39) contains site I; segment β (residues 40−75) contains site II; segment α′ (residues 76−112) contains site III; segment β′ (residues 113−148) contains site IV. The 12 residues of the calcium-binding sites (boxed residues) are aligned. The 5 residues monitored in these NMR spectroscopic studies are shown (white in a black box).

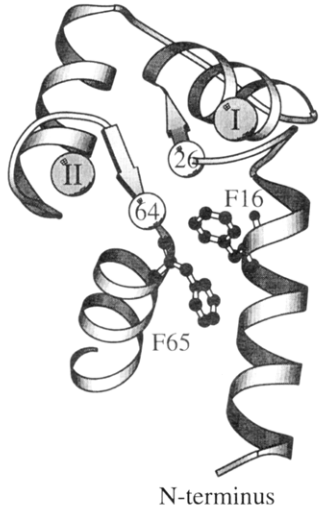

FIGURE 2: Depiction of calcium-saturated crystal structure (Babu *et al.*, 1988) of sites I and II in the N-terminal domain of calmodulin showing the positions monitored in the NMR during the equilibrium titrations. The side chains of the residues F16 and F65 are shown and labeled. The backbone α-carbon position of residues T26 and D64 is labeled. Drawing was made using MolScript (Kraulis, 1991).

0, 1, 2, 3, or 4 calcium ligands bound or (2) to monitor occupancy of each of the four calcium-binding sites as a function of calcium concentration. Rigorous, simultaneous determination of the occupancy of each of the sites of wild-type calmodulin under equilibrium binding conditions has eluded experimentalists for two decades.

It would be ideal to obtain individual-site binding isotherms such as those determined using NMR to monitor surface histidines of hemoglobin (Russu *et al.*, 1982) or DNase footprint titration methods to study repressor binding (Brenowitz *et al.*, 1986). Analysis of such isotherms (Ackers *et al.*, 1983) can yield the median free energy for ligand binding and estimates of the degree of heterogeneity (difference in intrinsic free energies) and cooperativity between sites. To do this, it is essential to monitor properties of the ligand or the macromolecule that reflect the number and position of ligands bound and not just the average degree of saturation of the population. It has been possible to study an intermediate of calbindin D_{9k} half-saturated by cadmium (Akke *et al.*, 1991); however, this was facilitated by one of the two sites having a pseudo-EF-hand (noncanonical) sequence and it is not possible to study either singly ligated intermediate species that is half-saturated with calcium.

A high degree of sequence homology makes the coordination geometry of each site of calmodulin very similar; thus, intermediates are difficult to distinguish. Although some metals, such as lanthanides, have spectral properties that depend on which of the four sites is occupied, they do not bind to the sites of calmodulin with the same order of preference as does calcium (Wang *et al.*, 1984). Therefore, they serve as poor models of the process of physiological activation of calmodulin. There are no spectral properties of calcium that vary depending on which site of calmodulin is occupied.

An alternative to monitoring site-specific properties of the ligand is to quantify properties of calmodulin that indicate occupancy of an individual site. The repeating nature of the calmodulin sequence complicates this approach to obtaining individual-site isotherms. Optical spectroscopy of vertebrate calmodulin is confounded by the near lack of spectroscopic probes; there are no tryptophan residues and only two tyrosine residues, both of which are in the C-terminal domain. Furthermore, most of the calcium-dependent changes in spectral signals (e.g., UV or fluorescence intensity) arise from changes in the environment of only one of these (Y138) which is in site IV (see Klevit, 1983 and Ross *et al.*, 1992 for reviews). Most experimental approaches can yield information about only the average binding properties of calmodulin or one of its domains.

Therefore, determination of individual-site binding isotherms for calmodulin requires the development of novel methodologies such as quantitative proteolytic footprinting studies (Pedigo & Shea, 1995; Verhoeven & Shea, 1993). Although the number of residues probed are few and specific to each protease, they are more widely distributed than tyrosine and may be identified unambiguously. These equilibrium studies of residue-specific conformational responses showed that the two domains of calmodulin interact over the course of binding four calcium ions; domain free energies and intradomain cooperativity also were estimated from these studies. A limitation of the proteolytic footprinting studies is that there are many regions of calmodulin that have not yet been monitored.

NMR provides an alternative approach to reveal residue-specific conformational changes in response to calcium binding to calmodulin (see Evans *et al.*, 1988 for review) and independently corroborate the findings from quantitative proteolytic footprinting studies. The repeating nature of the calmodulin sequence (Figure 1) and high helical content (Figure 2) contributes to severe spectral overlap. However, the ability to monitor a few residues unambiguously has shown that the isolated C- and N-terminal domains adopt structures very similar to those observed in whole calmodulin (Aulabaugh *et al.*, 1984; Ikura *et al.*, 1984; Dalgarno *et al.*, 1984) and that they retain most features of their global fold in the apo state (Ikura *et al.*, 1984, 1985; Hoffman & Klevit, 1991). These studies of isolated domains also facilitated assignment of resonances in whole calmodulin.

Stoichiometric binding studies monitored by 1-D NMR were the first to indicate several critical elements of the molecular mechanism of calcium binding to calmodulin. They showed that C-terminal domain sites have higher affinity for calcium than N-terminal domain sites, but that the chemical shifts of a few N-terminal domain residues

changed over the range of zero to two calcium ions per calmodulin (Seamon, 1980; Ikura *et al.*, 1983b, 1984; Klevit *et al.*, 1984; Urbauer *et al.*, 1995). These results could be interpreted as indicating that there is interdomain cooperativity or that the affinities of the domains are not completely separated in wild-type calmodulin. Stoichiometric titrations of reduced valency mutants of *Drosophila* calmodulin (Starovasnik *et al.*, 1992) clearly demonstrated site heterogeneity, and gave qualitative evidence for intra- and interdomain cooperativity. However, it is not possible to evaluate binding constants from stoichiometric binding studies alone.

This study of wild-type calmodulin was conducted under equilibrium, rather than stoichiometric, binding conditions in order to resolve the free energies of binding and cooperative interactions. However, the high concentration (~1 mM; 16 mg/ml) of calmodulin required for NMR experiments prevented a direct equilibrium titration because the K_d for calcium binding is in the micromolar range, three orders of magnitude lower than the protein concentration. To overcome this limitation of using NMR to evaluate the equilibrium thermodynamics of calcium binding, we employed the discontinuous titration approach developed in earlier quantitative proteolytic footprinting studies (Pedigo & Shea, 1995). Thus, the signal at each calcium concentration in these titrations represents the analysis of an individual sample of calmodulin extensively dialyzed to equilibrate it at an experimentally determined level of free calcium.

These titrations represent the first use of NMR spectroscopy to monitor calcium binding to calmodulin under *equilibrium* binding conditions. We have studied calcium binding at two concentrations of KCl to probe the site-specific electrostatic contributions to affinity and cooperative interactions among the four calcium-binding sites. We report binding free energies determined from model-dependent analysis of five binding isotherms for both sets of conditions.

EXPERIMENTAL PROCEDURES

Materials

Recombinant rat calmodulin in the T7-7 vector (Tabor & Richardson, 1985) was the kind gift of R. Mauer and P. Howard. It was overexpressed in *Escherichia coli* Lys-S cells (U.S. Biochemicals, Cleveland, OH), purified using phenyl sepharose CL-4B (Pharmacia, Piscataway, NJ) chromatography (Putkey *et al.*, 1985) and characterized as described previously (Pedigo & Shea, 1995). BAPTA and 4,4′-difluoro-BAPTA were purchased from Molecular Probes (Eugene, OR). Deuterium oxide (D_2O; 99.9%) was purchased from Cambridge Isotope Laboratories (Andover, MA). The chemical shift reference 3-(trimethylsilyl)propionate (TSP) was purchased from Aldrich Chemical Co. (Milwaukee, WI). Other routine laboratory chemicals were of the highest grade commercially available.

Methods

Calcium/pH Buffers. Calcium titrations of calmodulin were performed at two KCl concentrations. Buffers were either 50 mM HEPES, 92 ± 3 mM KCl, 0.5 mM sodium EGTA, and 0.5 mM sodium NTA (series A), or 10 mM HEPES, 152 ± 4 mM KCl, 50 μM sodium EGTA, and 5 mM sodium NTA (series B). The concentration of KCl was determined with a Radiometer CDM83 Conductivity Meter (Copenhagen). By the addition of calcium chloride, 15 distinct pCa buffers of series A and 16 distinct pCa buffers of series B were prepared to span a range of approximately nanomolar (pCa = 9) to millimolar (pCa = 3) free calcium concentration (where pCa denotes $-\log[Ca^{2+}]_{free}$). All buffers were pH 7.40 ± 0.01 at 22.0 °C.

Accurate knowledge of the free calcium concentration in the pCa/pH buffers required direct experimental determination. For buffers with high free calcium concentration (buffers in the pCa range 5.2 to 2.7) in each series, the free calcium was determined using a calcium-selective electrode as described previously (Pedigo & Shea, 1995). For buffers with low free calcium, this was determined by measuring the calcium-sensitive fluorimetric signal of 4 μM BAPTA (for buffers in pCa range below 6.4) or 4 μM difluoroBAPTA (buffers in pCa range 6.7 to 5.5) to determine their degree of saturation and using that value to calculate the pCa (Pedigo & Shea, 1995). The dissociation constants (K_d) for calcium binding to each of these fluorophores were determined in both buffers as described previously (Pedigo & Shea, 1995) except that the concentration of fluorophore was 1 μM. For buffer series A (92 mM KCl), the K_d was 1.26×10^{-7} M for BAPTA and was 1.83×10^{-6} M for difluoroBAPTA. For buffer series B (152 mM KCl), the K_d was 3.58×10^{-7} M for BAPTA and was 2.83×10^{-6} M for difluoroBAPTA. The buffers contained no added magnesium.

Equilibration of Calmodulin. Each of the pCa/pH/KCl buffers was used to equilibrate a 1 mL aliquot of calmodulin *via* extensive dialysis (using a membrane that retains proteins ≥10 kDa) so that a complete series of equilibrated samples was generated. The degree of saturation of the calcium-binding sites of calmodulin in the stock prior to dialysis was not determined. Equilibration was accomplished by four exchanges of buffer with a 1:80 volume ratio of dialysate: buffer at 4 °C and one exchange at ~22 °C. Dialysis conditions were sufficient to equilibrate calcium-saturated calmodulin to the pCa of the buffer. The final calmodulin concentration in the individual dialysates was determined with the BCA assay (Pierce, Rockford, IL) which had been calibrated with samples of calmodulin whose concentration had been determined by amino acid analysis; values varied between 7 and 14 mg/mL (420−840 μM). Dialysates were aliquotted and stored at −20 °C. For NMR studies, a 0.7 mL aliquot of each dialysate was dried in a Speed Vac concentrator (Savant, Farmingdale, NY) and reconstituted in 0.7 mL of D_2O at room temperature. The concentration of contaminating metals in the D_2O was not determined. Solutions were transferred into 5 mm glass NMR tubes (Wilmad Glass, Buena, NJ). Each titration required ~200 mg of calmodulin. A stock solution of TSP was prepared in water (500 mM) and stored at 4 °C. A 2 μL aliquot of this stock was added to each NMR sample for a final concentration of 1.4 mM TSP.

Calmodulin Fluorescence. The intrinsic tyrosine fluorescence of calmodulin was monitored in each of the individual calmodulin dialysates as described previously (Pedigo & Shea, 1995); dialysates were diluted 1:150 (v:v) in the corresponding pCa dialysis buffer prior to study. In order to correct for variations in the concentration of calmodulin in different dialysates, the tyrosine fluorescence of an individual dialysate was normalized to its endpoints of high and low fluorescence intensity as described previously (Pedigo & Shea, 1995).

NMR Data Acquisition. ^{1}H-NMR spectra were obtained at a frequency of 500 MHz on a Varian Unity 500 spectrometer at the University of Iowa College of Medicine NMR Facility. Both 1-D proton spectra and 2-D COSY spectra were obtained with pulse sequences furnished with the Varian instrument. All ^{1}H-NMR spectra of calmodulin dialysates at the 152 mM KCl were obtained by accumulation of 16 free induction decays (FID) using a 6.6 μs 90° pulse, a 2 s recycle delay, and spectral width of 6000 Hz. Each FID consisted of 8K data points; the frequency increment for each datum was the same in all experiments. Longitudinal relaxation times for aromatic protons were determined experimentally. Long T_1 values ($\leq$3.8 s) dictated use of long recycle delays. Thus, parameters for acquisition of the 92 mM KCl data were adjusted to include a delay of 23 s between 90° pulses. A subset of samples from buffer series B (152 mM KCl) were analyzed at these longer delay times. No change in the relative areas of aromatic resonances was observed. For analysis of all calmodulin dialysates, the residual HDO peak was suppressed by preirradiation for 1 s prior to the 90° pulse. Chemical shifts were measured in parts per million (ppm) from an internal standard of TSP at 0 ppm. Temperature during acquisition was monitored at 22 $\pm$ 2 °C. Peak shape and chemical shift were found invariant over this temperature range.

At some pCa levels, there was significant overlap of resonances such that the chemical shifts of F16 and F65 were not well resolved; for those dialysates, COSY spectra also were acquired in order to confirm the assignments. The acquisition parameters were the same as for the 1-D spectra described previously except that the number of points was decreased to 2048 in the F2 dimension and was 256 in the F1 dimension. The number of transients was 8 and the delay between transients was 4 s.

Processing. All 1-D spectra were analyzed using FELIX (v. 1.1; Hare Research, Woodinville, WA). Exponential apodization was used with a line broadening parameter of 2 Hz. Spectra were phased and base line corrected. Hewlett Packard plotter files created in FELIX were converted to an (X,Y) coordinate format suitable for analysis by PEAKFIT (Jandel Scientific, Corte Madera, CA). (The conversion of each of the 8000 data points of each FID to a chemical shift value required selecting the TSP maximum from the (X,Y) coordinate file and assigning that position to be zero.) The resonance area and chemical shift for $F16_{C\delta H}$, $T26_{C\alpha H}$, $D64_{C\alpha H}$, $F65_{C\delta H}$, $H107_{C\delta H}$, $Y138_{C\delta H}$, and $Y138_{C\epsilon H}$ were determined using PEAKFIT by manual fitting of a Gaussian or Lorentzian function. The reproducibility of this procedure will be described below. Resonance assignments were based on reported values (Hoffman & Klevit, 1991; Dalgarno *et al.*, 1984; Ikura *et al.*, 1985); in no case were the assignments ambiguous. Aromatic spin systems for assigned resonances were identified in the COSY spectra.

Resolution of Calcium-Binding Isotherms. Resonances that were in fast exchange on the time scale of the NMR experiment were followed by monitoring the change in their chemical shift as a function of calcium concentration in the dialysate. Resonances that were in slow exchange were followed by monitoring the change in normalized resonance area. This report includes only well-resolved and unambiguously identified resonances that were followed throughout titrations at both levels of KCl.

The titrations spanned a pCa range from 9 (apo) to 3 (fully saturated). In the N-terminal domain, changes in chemical shift were monitored for the resonances of $F16_{C\delta H}$, $F65_{C\delta H}$, $T26_{C\alpha H}$, and $D64_{C\alpha H}$, which were in fast exchange on the time scale of the NMR experiment. At intermediate calcium concentrations, it was assumed that the chemical shift value represented a weighted average of the fractions of the endstates of the domain (apo- and calcium-saturated). The error in the chemical shift value was determined to be smaller than 0.01 ppm as evaluated by several methods including comparison of duplicate spectra of the same dialysate. In addition, the standard deviation of the average chemical shift for dialysates representing the asymptotes of the isotherms was found to be ~0.003 ppm, significantly less than 0.01 ppm. In addition, we evaluated the error that processing by PEAKFIT introduced into the determinations of resonance area and position by using a Gaussian function to fit a single spectrum in triplicate. Although the position resolved for the chemical shift maximum was found to be invariant, the area of the resonances determined in this way varied among the triplicate determinations.

Procedures for manually determining the position of the maximum of the TSP resonance have the potential to introduce significant error in the values of chemical shift from this reference. In experiments reported here, the position of the maximum of the TSP peak was determined numerically as described earlier; however, the data point at which this maximum occurred was not identical in all spectra. As an additional indication of the possible error in the chemical shift values, we determined that the TSP maximum was datum 7207($\pm$3) for all dialysates at 152 mM KCl. If the same uncertainty exists in determining the position of the maximum of the resonances of calmodulin, that corresponds to a possible total error of 6 points in 8000 or 0.009 ppm in the determination of the chemical shift. Thus, the precision in the determination of the chemical shift values for $F16_{C\delta H}$, $F65_{C\delta H}$, $T26_{C\alpha H}$, and $D64_{C\alpha H}$ was estimated as being 0.01 ppm at worst.

In order to evaluate the effect of this level of uncertainty in the resolution of binding isotherms from calcium-dependent changes in the chemical shift values, each experimentally resolved signal (S_{exptl}) was perturbed by an absolute error (offset = β) in the range of $\pm$0.01 ppm according to eq 1.

$$S' = S_{exptl} + \beta \quad (1)$$

Random values of β between 0 and 0.010 were generated by EXCEL (Microsoft Corp., v. 4 for Macintosh) and were either added or subtracted from the experimental data based on whether the final digit was even or odd. This procedure was used to create three distinct sets of error-perturbed binding isotherms that were analyzed in the same way as the experimental data sets, as described below.

The resonance for $Y138_{C\delta H}$ at 6.32 ppm and $H107_{C\delta H}$ at 7.78 ppm were well resolved from other resonances in spectra at both concentrations of KCl. The resonance for $Y138_{C\delta H}$ at 6.32 ppm was integrated by manual fitting of a Gaussian function as described above. The integration of $H107_{C\delta H}$ at 7.78 ppm was not as straightforward because its shape varied over the course of the calcium titration. This has been noted previously (Starovasnik *et al.*, 1992). For example, at 92 mM KCl and free calcium of 6.31×10^{-7} M, the $H107_{C\delta H}$

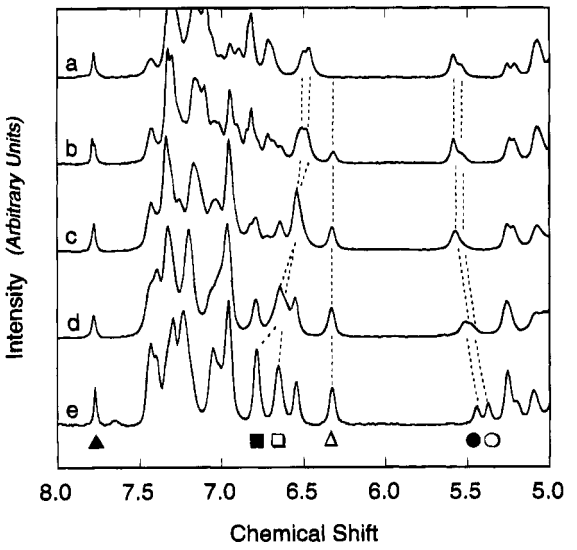

FIGURE 3: Aromatic and CαH region (8−5 ppm) of spectra in a calcium titration of calmodulin. The free calcium concentration for each spectrum is (a) 1×10^{-9} M, (b) 6.31×10^{-7} M, (c) 2.82×10^{-6} M, (d) 3.98×10^{-6} M, and (e) 1.70×10^{-4} M in 50 mM HEPES, 92 mM KCl, pH 7.4 @ 22 °C. Slow exchange behavior was apparent for $Y138_{C\delta H}$ at 6.32 ppm (Δ). Fast exchange behavior was apparent for resonances $F16_{C\delta H}$ (□; 6.51 (apo) to 6.65 ppm for calcium-saturated CaM), $T26_{C\alpha H}$ (○; 5.54−5.38 ppm), $D64_{C\alpha H}$ (●; 5.59−5.45 ppm), and $F65_{C\delta H}$ (■; 6.47−6.79 ppm). Spectra were normalized to the area 1 proton represented by area of $H107_{C\delta H}$ (▲) at 92 mM KCl or half the area of the sum of $T26_{C\alpha H}$ and $D64_{C\alpha H}$ at 152 mM KCl.

resonance appeared as two distinct resonances indicating that this proton was in slow chemical exchange (Figure 3b); thus, the $H107_{C\delta H}$ resonance was integrated as 2 Lorentzian functions and the sum was taken to represent one proton. In order to resolve a binding isotherm, the number of protons represented by the $Y138_{C\delta H}$ resonance at 6.32 was determined by dividing the area of $Y138_{C\delta H}$ by the area of $H107_{C\delta H}$ for each dialysate. These ratios were plotted as a function of free calcium concentration in the dialysate for the data in 92 mM KCl; at saturating concentations of free calcium, the ratio was 1.87 ± 0.06 protons.

Note that regardless of shape, the area of peaks attributed to $H107_{C\delta H}$ should represent one proton as long as no other protons contribute to these peaks. This assumption was supported for the titrations at 92 mM KCl by comparing the area of $H107_{C\delta H}$ to that of half the sum of areas for two protons ($T26_{C\alpha H}$ and $D64_{C\alpha H}$) that were in fast exchange. However, this was not the case for the titrations in 152 mM KCl.

The relative area of $Y138_{C\delta H}$ to $H107_{C\delta H}$ at saturating calcium was less than two protons (~1.4 protons) in buffer series B (152 mM KCl). Upon inspection of the spectra, it was evident that this discrepancy resulted from the area of $H107_{C\delta H}$ being large relative to the areas of other resonances in the aromatic region that represented one proton. Thus, in analysis of spectra of calmodulin in buffer series B (152 mM KCl), half of the area of the overlapping peaks corresponding to $T26_{C\alpha H}$ and $D64_{C\alpha H}$ (representing two protons) was used as an alternative to $H107_{C\delta H}$ as a standard for the area of one proton. Normalized data for $Y138_{C\delta H}$ were plotted as a function of free calcium concentration in the dialysate; at saturating concentations of free calcium, the ratio was 1.99 ± 0.08 protons.

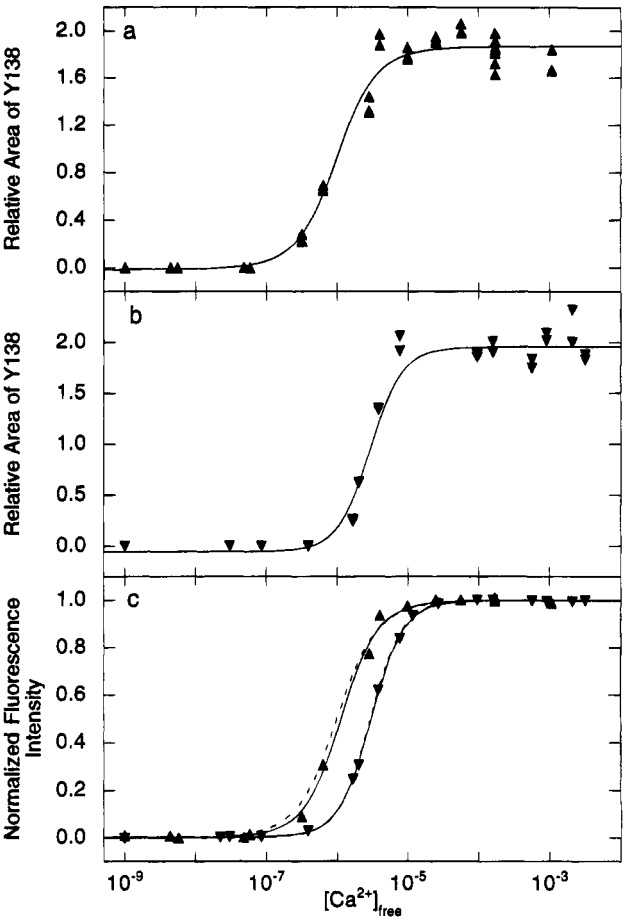

FIGURE 4: Calcium titrations of calmodulin monitored as the change in $Y138_{C\delta H}$ resonance area or tyrosine fluorescence. Signal plotted against the free calcium concentration (M) in each dialysate. (a) At 92 mM KCl, $Y138_{C\delta H}$ resonance area (▲; normalized against area of $H107_{C\delta H}$); curve simulated with parameters in Table 1. (b) At 152 mM KCl, $Y138_{C\delta H}$ resonance area (▼; normalized against half of the sum of areas of $T26_{C\alpha H}$ and $D64_{C\alpha H}$); curve simulated with parameters in Table 1. All duplicate analyses are plotted; however, data pairs between pCa 9 and 5 overlay closely. (c) Normalized intrinsic tyrosine fluorescence at 92 mM KCl (▲) and 152 mM (▼). Solid curves simulated with parameters in Table 1 resolved from fits of fluorescence data; dashed curves simulated with parameters resolved from fits of NMR data (identical to solid curves in panel a and b) are shown for ease of comparison.

This ratio is sensitive to error in the determination of the area of the standard as well as the resonance of interest. In order to evaluate the precision in the determination of the relative area of $Y138_{C\delta H}$, each spectrum was integrated twice using PEAKFIT with manual adjustments of the base line; this appears to be the source of greatest error in the analysis of a resonance in slow exchange. Both determinations of relative areas of peaks were included in isotherms (see Figure 4) and model-dependent analysis of the data at each pCa (Table 1). The precision of integrating replicate spectra of the same dialysate was determined to be within the precision of duplicate integrations of a single spectrum.

Data Analysis. Isotherms resolved from NMR and fluorescence signals were fit using NONLIN (Johnson & Frasier, 1985) running on a Silicon Graphics Personal Iris workstation; Fortran functions were written to correspond to the following equations, except that binding constants were expressed in the form of free energies. The concentration of free calcium in each dialysate (the independent variable) was assumed to be known precisely. For estimation of

parameters, we assumed the experimental signal (ppm, normalized resonance area or fluorescence signal) to be linearly related to the fractional saturation of the corresponding domain. Problems with this convention have been described previously (Pedigo & Shea, 1995) and considerations specific to these NMR data will be discussed here.

In order to determine the total free energies of calcium binding and estimates of the cooperative interactions between the sites in a domain, the data were fit to two simple binding models. Model I (eq 2) treated sites as homogeneous (equal intrinsic affinities) and independent (noncooperative); average fractional saturation of both sites was given by

$$\bar{Y}_I = \frac{K_1[X]}{1 + K_1[X]} \quad (2)$$

where the fractional saturation is the ratio of the occupied sites to the total number of sites. According to this model, K_1 represents the intrinsic association constant for a site (k_1) and [X] is the concentration of free calcium in the dialysate. The total free energy of calcium binding to the domain would be twice the value of ΔG_1 ($-RT \ln K_1$). Model II (eq 3; standard Adair equation for two sites) allowed the pair of sites to be heterogeneous and cooperative.

$$\bar{Y}_{II} = \frac{K_1[X] + 2K_2[X]^2}{2(1 + K_1[X] + K_2[X]^2)} \quad (3)$$

The equilibrium constant K_1 represents the sum of two intrinsic equilibrium constants (k_1 and k_2) that are not necessarily equal. The parameter K_2 represents the equilibrium constant ($k_1k_2k_{12}$) for binding ligand to both sites; it accounts for any positive or negative cooperativity ($k_{12} \neq 1$) regardless of its source or magnitude. It is not possible to determine analytically the intradomain cooperativity, k_{12}, from these data alone; it may be estimated by assuming that the binding sites have equal intrinsic affinities ($K_1 = k_1 + k_2 = 2k$ and $K_2 = k_1k_2k_{12} = k^2k_{12}$). This leads to eq 4, which gives a lower limit (K_c) on the true value of cooperativity (k_{12}).

$$K_c = \frac{4K_2}{K_1^2} \quad (4)$$

To accommodate the experimental data without prior normalization, the function (f(X)) used for fitting the data to each model was

$$f(X) = Y_{[X]_{low}} + \bar{Y}_j \times \text{Span} \quad (5)$$

where $\bar{Y}_j$ refers to average fractional saturation in model I or II as defined by eqs 2 or 3. Note that the value of the parameter $Y_{[X]_{low}}$ corresponds to the value of the dependent variable (experimental spectroscopic signal) at the lowest calcium concentration in the titration and that the value of the parameter Span is positive for a monotonically increasing signal. At the limit of saturating ligand concentration ($\bar{Y}_j = 1$), the experimental signal is equal to the sum of these two parameters.

Model-dependent analyses of the spectroscopic transitions representing each calcium titration were conducted exhaustively over a wide range of starting guesses for all parameters.

Table 1: Model-Dependent Analyses[a] of Calmodulin Titrations Monitored by Fluorescence and NMR of Y138[b]

data[b]	[KCl], mM	ΔG_1[c]	ΔG_2	$\sqrt{\text{var}}$[d]	ΔG_c[e]
Tyr Fluor.[f]	92	-7.49 ± 0.62	-16.07 ± 0.16	0.024	$-1.9\ ^{-1.2}_{+1.3}$
$Y138_{C\delta H}$[g]	92	-7.80 ± 0.97	-16.22 ± 0.24	0.134	$-1.4\ ^{-1.9}_{+0.8}$
Tyr Fluor.	152	-6.05 ± 0.66	-14.91 ± 0.24	0.062	$-3.6\ ^{-1.3}_{+0.6}$
$Y138_{C\delta H}$[h]	152	*(−6.05)*	-14.95 ± 0.16	0.143	-3.7 ± 0.2

[a] Model II (eq 3) allowed heterogeneous and cooperative binding. [b] Data spanned a free calcium range of 1 nM to 2.1 mM (pCa = 9.0−2.68). [c] All free energies are expressed in kcal/mol (1 kcal = 4.184 J). To overestimate the uncertainty, the greater of the positive or negative limit of each asymmetric 65% confidence interval was tabulated. [d] Correlation coefficients and the magnitude and distribution of residuals were evaluated but not shown; for all data sets, fits to model I showed nonrandom residuals. [e] Estimate of cooperative free energy was calculated as $\Delta G_c = -RT \ln 4 + \Delta G_2 - 2\Delta G_1$; this formulation assumes that the intrinsic binding energies are equal and gives a lower limit of the actual cooperativity. [f] Tyrosine fluorescence. [g] $Y138_{C\delta H}$ resonance integrated to 1.87 ± 0.06 protons in calcium-saturated calmodulin when normalized against $H107_{C\delta H}$. [h] $Y138_{C\delta H}$ resonance integrated to 1.99 $\pm$ 0.08 protons in calcium-saturated calmodulin when normalized against half the sum of areas for $T26_{C\alpha H}$ and $D64_{C\alpha H}$. Value of ΔG_1 in parentheses was fixed for this fit.

In addition, multiple combinations of numerical constraints were applied to the free energies and normalization parameters. In all but one of the fits reported, both association free energies (ΔG_1, ΔG_2) were floated parameters; in all but two cases (the data for $F16_{C\delta H}$ in the titration at 92 mM KCl and the data for $Y138_{C\delta H}$ in the titation at 152 mM KCl), it was possible to solve simultaneously for both endpoint parameters ($Y_{[X]_{low}}$ and Span) as well as the free energies of binding (see footnotes to the tables).

Multiple criteria were used for evaluating goodness-of-fit for the best-fit parameters in each case. As reported by NONLIN, these error statistics included (a) the value of the square root of variance, (b) the values of asymmetric 65% confidence intervals, (c) the distribution of residuals, (d) the magnitude of the span of residuals, and (e) the absolute value of elements of the correlation matrix. The values of ΔG_c (from eq 4) and propagated confidence intervals were estimated by NONLIN using the best-fit values for ΔG_1 and ΔG_2 determined in each individual fit to model II (eqs 3 and 5).

RESULTS AND DISCUSSION

The goal of these studies was to apply NMR spectroscopy to monitor calcium-dependent structural changes of calmodulin over the course of an *equilibrium* titration and thereby determine individual-site binding isotherms. It is generally not possible to use NMR to monitor equilibrium titrations of high affinity ligand binding because the concentration of macromolecule required for sufficient signal intensity exceeds the ligand dissociation constant by several orders of magnitude. This would limit the investigation to stoichiometric binding properties; although such studies are very informative, they do not permit estimation of free energies of binding and interaction. We overcame this limitation by conducting a discontinuous equilibrium titration, an approach that had been used successfully in quantitative proteolytic footprinting studies of calmodulin titrations (Pedigo & Shea, 1995; Verhoeven & Shea, 1993). Those prior equilibrium studies and the NMR studies reported here offer the advantage of monitoring residue-specific confor-

mational change in both the N- and C-terminal domain simultaneously. Equilibrium calcium binding properties of the N-terminal domain cannot be monitored easily in wild-type vertebrate calmodulin because there are no optical spectroscopic probes in that domain.

1-D Proton NMR of Calmodulin. Calmodulin was equilibrated in discrete pCa/pH buffered solutions in which the concentration of free calcium had been determined experimentally. Calcium-dependent changes of resonances in 1-D proton NMR spectra were used to create calcium-binding isotherms for five residues; each datum in a titration curve resulted from analysis of an individual dialysate of calmodulin at a distinct pCa. Model-dependent analysis of these isotherms yielded estimates of the microscopic binding energies of calmodulin.

Because calmodulin is predominantly helical and has a repetitive amino acid sequence (Figures 1 and 2), there is a high degree of overlap in the 1-D proton NMR spectrum (cf., Wishart *et al.*, 1991). Figure 3 shows five spectra from dialysates that spanned a range from apo (Figure 3a) to calcium-saturated (Figure 3e) calmodulin. The spectra show that there was significant spectral overlap in the region from 8 to 6.3 ppm, with contributions from eight phenylalanine, one histidine, and two tyrosine residues. Using assignments made by others (see Experimental Procedures), six resonances were monitored unambiguously in spectra for all dialysates of these discontinuous calcium titrations. Slow exchange behavior was monitored for the resonances of $H107_{C\delta H}$ and $Y138_{C\delta H}$ in the C-terminal domain. Fast exchange behavior was monitored for the resonances of $F16_{C\delta H}$, $T26_{C\alpha H}$, $D64_{C\alpha H}$, and $F65_{C\delta H}$ in the N-terminal domain. The observed exchange behavior was consistent with the relative calcium affinities of the domains and calcium off-rates as have been determined by NMR (Ikura, 1986; Tsai *et al.*, 1987) and stopped flow studies (Bayley *et al.*, 1984; Martin *et al.*, 1985; Teleman *et al.*, 1986).

Calcium-Binding to the C-Terminal Domain. The δ-proton resonances for $Y138_{C\delta H}$ existed as a pair whose intensity changed reciprocally (increased at 6.32 ppm (Δ) or decreased at 6.72 ppm; see Figure 3) over the course of the titration. At intermediate calcium concentrations (near pCa 6), there were two distinct resonances for configurationally equivalent protons. Because of spectral overlap, only the resonance of $Y138_{C\delta H}$ at 6.32 ppm was integrated accurately throughout the titrations. The complementary resonance for $Y138_{C\delta H}$ (at 6.72 ppm for apocalmodulin) and the pair of resonances for $Y138_{C\epsilon H}$ (at 6.55 ppm for Ca^{2+}-bound and at 6.70 ppm for apocalmodulin) were identified but not integrated in all of the 1-D and 2-D spectra.

In all spectra comprising the titration at 92 mM KCl, the resonance area of the $Y138_{C\delta H}$ resonance at 6.32 ppm (Ca^{2+}-bound) was normalized to the area of $H107_{C\delta H}$ at 7.78 ppm (Figure 4a) to account for differences in the calmodulin concentration in each dialysate. The area for the $Y138_{C\delta H}$ resonance normalized to 1.87 protons, close to the expected value of 2. In all spectra comprising the titration at 152 mM KCl, $Y138_{C\delta H}$ data were normalized to half of the sum of $T26_{C\alpha H}$ and $D64_{C\alpha H}$ (Figure 4b) as described in Experimental Procedures. The area for the $Y138_{C\delta H}$ resonance normalized to 1.99 protons. Calcium-binding isotherms were constructed from the normalized resonance area at each level of pCa for the titrations in the 92 mM (Figure 4a) and 152 mM KCl buffers (Figure 4b). Affinity of calmodulin for calcium was higher in 92 mM KCl than in 152 mM KCl. Table 1 lists parameters resolved from model-dependent analysis of the calcium-binding isotherms resolved from the NMR study of $Y138_{C\delta H}$ in 92 and 152 mM KCl. There is significant scatter in the duplicate data points at each level of pCa because they represent the ratio of two areas, bothof which may have significant error whose major source is the assignment of the base line.

Calcium-sensitive changes in the environment of Y138 also may be monitored by fluorescence intensity, which offers an opportunity to compare isotherms resolved by independent methods. The normalized tyrosine fluorescence of each of the dialysates is shown in Figure 4c. The most striking aspect of these titrations is the similarity of the best fit curves (compare dashed and solid curves in Figure 4c) that resulted from analysis of the same calmodulin dialysates using techniques that require very different manipulations and methods of data reduction and normalization. Given that significant error could have been introduced by either the NMR or fluorescence approaches, the agreement indicates that the resolved isotherms represent the same properties of Y138. However, given that the response of Y138 changes over the entire course of binding four calcium ions to calmodulin (see Ross *et al.*, 1992 for review and Pedigo & Shea, 1995 for discussion), the isotherms may have contributions from binding at sites in the N-terminal domain, as well as from sites III and IV.

The values of binding free energies and estimates of lower limits of the cooperativity for calcium binding to the C-terminal domain resolved from fits of the fluorescence and NMR data to model II are listed in Table 1. In all cases, the data were fit better by model II (eq 3), which allowed for heterogeneous and cooperative binding. At each KCl concentration, analysis of fluorescence and $Y138_{C\delta H}$ isotherms yielded very similar values of total free energy (ΔG_2); for titrations at 92 mM KCl, the values reported here are in excellent agreement with those resolved from fluorescence and quantitative proteolytic footprinting studies of the same samples reported previously (Pedigo & Shea, 1995). Resolution of the total free energy and fitted endpoints of the data for $Y138_{C\delta H}$ at 152 mM KCl required that the parameter ΔG_1 be fixed; its value was held at the value of ΔG_1 determined in the corresponding fit of the fluorescence data. As is evident in Figure 4b, there is a small systematic deviation between the NMR data and the simulated isotherm, such that the data appear more cooperative. Thus, the lower limit of the intradomain cooperativity (ΔG_c) determined from the fluorescence experiment is a more reliable estimate than that determined from the NMR experiment.

As expected, the calcium binding affinity of calmodulin was lower in higher salt. Although potassium is recognized to diminish the calcium binding affinity of calmodulin, the molecular origins of this effect have not been fully established. With an experimentally determined pI of 3.92, calmodulin is predicted to be negatively charged at pH 7.4 and potassium is expected to shield negative charges, perhaps competing directly for residues that would participate in calcium chelation. From the line widths of α-carbon and amine protons in NMR spectra of calmodulin in the presence and absence of K^+, Linse *et al.* (1991) concluded that the effect of K^+ was due to nonspecific screening of charged groups on the surface of calmodulin. This conclusion is also consistent with the experimental and theoretical studies of

electrostatic effects by Svensson *et al.* (1993). On the basis of equilibrium dialysis studies of salt-dependent binding of calcium to calmodulin, Haiech *et al.* (1981) proposed that K^+ competes with Ca^{2+} for the calcium-binding sites. Near UV circular dichroism studies of bovine calmodulin (Crouch & Klee, 1980) showed that there is a change in the spectrum (and therefore secondary and/or tertiary structure) upon addition of K^+; however, a larger change occurred after the subsequent addition of calcium, suggesting that potassium does not completely mimic calcium.

Despite the less favorable binding free energies at a higher salt concentration, the calculated values of ΔG_c were more favorable for binding (more negative). As mentioned previously, the propagated errors on the calculation of ΔG_c are large. However, because the confidence intervals on the ΔG_c values for the fluorescence experiments overlap by only 0.1 kcal/mol, we conclude that the numerical difference in cooperativity calculated for the two salt concentrations probably indicates a real chemical difference. This salt-dependent change is consistent with similar values of ΔG_c that may be calculated from macroscopic binding energies derived from equilibrium dialysis studies (Crouch & Klee, 1980) and competition studies with a chromophoric chelator (Linse *et al.*, 1991). These studies indicated an apparent increase in intradomain cooperativity with an increase in KCl concentration. However, it is important to emphasize that the calculation of K_c (eq 4) assumes that the sites are homogeneous and hence gives only an estimate of the lower limit of the actual cooperativity. An increase in K_c may reflect a decrease in the heterogeneity of intrinsic site affinities rather than an increase in cooperativity.[2]

In principle, the degree of heterogeneity for a two site macromolecule can be assessed experimentally by simultaneous analysis of (a) pairs of individual-site isotherms (Ackers *et al.*, 1983) or (b) the fractional population of three individual ligation species (cf., Senear & Brenowitz, 1991). However, for monitoring calcium binding to the C-terminal domain of calmodulin by NMR or fluorescence, there is only one signal (Y138); thus, we cannot determine unique values for the microscopic equilibrium constants for binding and cooperativity. Because the intrinsic affinities of the four calcium-binding sites in calmodulin are not known, the actual values of intradomain cooperativity cannot be determined from these analyses alone. In the following discussion of signals from the N-terminal domain, we consider other factors that may contribute to the shape of the titration curves as resolved from NMR spectra.

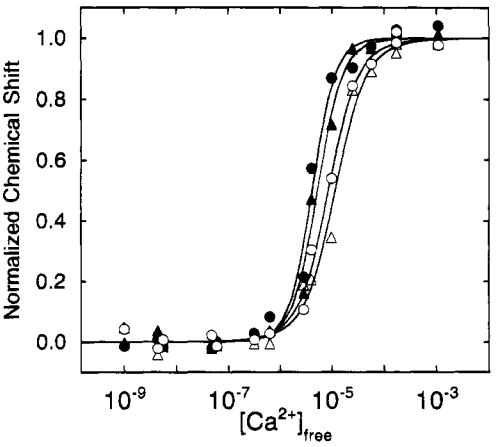

FIGURE 5: Calcium titration of calmodulin in 92 mM KCl buffer. Calcium-dependent changes in normalized chemical shift of resonances for $F16_{C\delta H}$ (●), $F65_{C\delta H}$ (▲), $T26_{C\alpha H}$ (○), and $D64_{C\alpha H}$ (△) *vs* the free calcium concentration (M) in each dialysate. Curves simulated with parameters resolved from best fits to model II (Table 2).

Calcium Binding to the N-Terminal Domain. Resonances resulting from $F16_{C\delta H}$, $T26_{C\alpha H}$, $D64_{C\alpha H}$, and $F65_{C\delta H}$ were monitored at each pCa; as seen in Figure 3, the phenylalanine side chain δ-proton resonances shifted downfield from 6.51 to 6.65 ppm ($\Delta = 0.14$ ppm) for F16 (□) and from 6.47 to 6.79 ppm ($\Delta = 0.32$ ppm) for F65 (■). Thus, the magnitude of the change in the chemical shift observed for $F65_{C\delta H}$ was approximately twice that observed for $F16_{C\delta H}$. The Cα backbone protons (in the β-sheet region of sites I and II) shifted upfield from 5.54 to 5.38 ppm ($\Delta = -0.14$ ppm) for T26 (○) and from 5.59 to 5.44 ppm ($\Delta = -0.15$ ppm) for D64 (●). The direction of the change for the backbone resonances was opposite that for the side-chain resonances but similar in magnitude to that observed for F16. The disposition of these residues in a crystal structure of calcium-saturated calmodulin (Babu *et al.*, 1988) is shown in Figure 2. In site I, T26 is in the first position of the antiparallel β-sheet region, facing D64 in the third position of the complementary β-sheet region of site II; they are not directly hydrogen bonded (Babu *et al.*, 1988). Their resonances are known to be sensitive to the conformation of both of the paired sites in this domain (Starovasnik *et al.*, 1992).

Of the side chain CδH resonances monitored, F16 is in the helix leading into site I and F65 (next to D64) is in site II and located adjacent to, but not in, the β-sheet region. In crystallographic studies of calcium-saturated calmodulin, F16 and F65 were observed to be in close proximity with their rings oriented perpendicularly (Babu *et al.*, 1988). In NMR studies of both apo (Ikura *et al.*, 1983a) and calcium-saturated calmodulin (Dalgarno *et al.*, 1984), there are NOEs observed between these residues as well as between F16 and I27, in the β-sheet region next to T26. Both F16 and F65 contribute to a region of aromatic residues in the N-terminal domain termed the "Phe-box" (Klevit *et al.*, 1984) and are not a part of the hydrophobic cleft *per se*.

For the calcium titration at 92 mM KCl, Figure 5 shows the isotherms resolved from the chemical shifts of $F16_{C\delta H}$, $T26_{C\alpha H}$, $D64_{C\alpha H}$, and $F65_{C\delta H}$. As is apparent upon visual inspection of Figure 5, the isotherms split into two classes.

[2] In the absence of direct estimates of intrinsic equilibrium constants (k_1 and k_2), we can consider some limiting cases. By rearranging the expression for K_c, the apparent equilibrium constant for cooperativity, in terms of a heterogeneity ratio k_h ($= k_1/k_2$, where $k_h \geq 1$ by definition) we obtain the following expression for K_c in terms of k_h, and the cooperativity, k_{12}.

$$K_c = k_{12}\frac{4k_h}{(1 + k_h)^2} \quad (6)$$

As required, this expression reduces to $K_c = k_{12}$ for sites of equal intrinsic affinity ($k_h = 1$). However, $K_c < k_{12}$ for heterogeneous sites and thus provides a lower limit on an estimate of the actual cooperativity constant (k_{12}). The compensatory contributions of cooperativity and heterogeneity are such that for the *same* cooperative interaction (i.e., k_{12} constant), the value of K_c will increase if there is a decrease in heterogeneity between sites (i.e. smaller value of k_h); for a 10-fold difference in intrinsic affinity, $K_c = 0.33k_{12}$, while a 2-fold difference yields $K_c = 0.89k_{12}$. Note that the value of K_c (a) cannot indicate positive cooperativity if there is none, and (b) is necessarily < 1 (i.e., indicates apparent anticooperativity) if the sites are both noncooperative (i.e., $k_{12} = 1$) and also heterogeneous.

Table 2: Model-Dependent Analyses[a] of Calmodulin Titrations[b] Monitored by NMR of N-Terminal Domain Residues

proton	[KCl], mM	ΔG_1[c]	ΔG_2	$\sqrt{\text{var}}$[d]	ΔG_c[e]
$T26_{C\alpha H}$	92	-6.46 ± 0.51	-13.35 ± 0.30	0.008	$-1.2\ ^{-2.5}_{+1.0}$
$D64_{C\alpha H}$	92	-6.55 ± 0.39	-13.70 ± 0.20	0.005	-1.4 ± 1.4
$F65_{C\delta H}$	92	-6.15 ± 1.25	-14.27 ± 0.20	0.014	$-2.8\ ^{-\infty}_{+1.9}$
$F16_{C\delta H}$[f]	92	-6.53 ± 0.69	-14.52 ± 0.14	0.008	$-2.3\ ^{-\infty}_{+1.3}$
$T26_{C\alpha H}$	152	-5.98 ± 0.24	-12.37 ± 0.12	0.003	-1.2 ± 0.5
$D64_{C\alpha H}$	152	-5.92 ± 0.29	-12.53 ± 0.11	0.003	-1.5 ± 0.6
$F65_{C\delta H}$	152	-6.29 ± 0.40	-12.83 ± 0.19	0.010	-1.1 ± 0.8
$F16_{C\delta H}$	152	-6.17 ± 0.64	-13.09 ± 0.16	0.004	-1.6 ± 1.3

[a] Model II (eq 3) allowed heterogeneous and cooperative binding. [b] Data spanned a free calcium range of 1 nM to 2.1 mM (pCa = 9.0–2.68). [c] All free energies are expressed in kcal/mol (1 kcal = 4.184 J). To overestimate the uncertainty, the greater of the positive or negative limit of each asymmetric 65% confidence interval was tabulated. [d] Correlation coefficients and the magnitude and distribution of residuals were evaluated but not shown; for all data sets, fits to model I showed nonrandom residuals. [e] Estimate of cooperative free energy was calculated as $\Delta G_c = -RT \ln 4 + \Delta G_2 - 2\Delta G_1$. Confidence intervals were propagated by NONLIN; the value of infinity (∞) indicates that this confidence interval was not defined. [f] Endpoints were fixed in fits of these data.

Table 3: Model-Dependent Analyses[a] of Error-Perturbed Calmodulin Titrations[b] of N-Terminal Domain Residues

proton	[KCl], mM	ΔG_2[c]	ΔG_c[d]
$T26_{C\alpha H}$	92	-13.40 ± 0.10	-1.9 ± 0.9
$D64_{C\alpha H}$	92	-13.67 ± 0.17	-1.5 ± 0.7
$F65_{C\delta H}$	92	-14.30 ± 0.03	-3.2 ± 0.1
$F16_{C\delta H}$	92	-14.51 ± 0.03	-3.2 ± 1.5
$T26_{C\alpha H}$	152	-12.30 ± 0.14	-1.7 ± 0.4
$D64_{C\alpha H}$	152	-12.51 ± 0.06	-1.5 ± 0.6
$F65_{C\delta H}$	152	-12.79 ± 0.09	-1.1 ± 0.2
$F16_{C\delta H}$	152	-13.13 ± 0.09	-2.0 ± 1.1

[a] Model-dependent analysis of error-perturbed data was performed as described in Experimental Procedures. Values resolved for ΔG_1 are omitted for clarity. [b] Experimental NMR chemical shift data for N-terminal domain resonances were perturbed by random values in the range of ±0.01 ppm. [c] Free energies are expressed in kcal/mol (1 kcal = 4.184 J). The error reported for these values is the standard deviation in the average of six values (parameters resolved from fits with fixed and floated endpoints for each of three error-perturbed data sets). [d] Only fits with floated endpoints were averaged because of the sensitivity of ΔG_c to the span of the data.

The isotherms defined by side-chain resonances ($F16_{C\delta H}$ and $F65_{C\delta H}$) had a lower median ligand activity (indicating higher affinity binding) than those of the backbone protons ($D64_{C\alpha H}$ and $T26_{C\alpha H}$). In addition, the isotherms for $F16_{C\delta H}$ and $F65_{C\delta H}$ represent an apparently more cooperative binding transition than those for $D64_{C\alpha H}$ and $T26_{C\alpha H}$. As described in Experimental Procedures, these data were treated as representing the average degree of saturation of the N-terminal domain and analyzed according to eq 5. The parameters ΔG_1, ΔG_2, $Y_{[X]_{low}}$, and Span were fit simultaneously with only one exception; best-fit values are listed in Table 2. In every case, model II was superior to model I as evaluated by inspection of residuals (not shown), confidence intervals, and the square root of the variance. The resolved values of the total free energy (ΔG_2) for F16 and F65 were distinct from those resolved for T26 and D64. (The members of these pairs were judged to be indistinguishable because their confidence intervals for ΔG_2 overlap.) Thus, the backbone and side-chain resonances appear to monitor binding transitions that differ in terms of both affinity and possibly cooperativity.

The calculated values for intradomain cooperativity (ΔG_c) are reported in Table 2. The values for ΔG_c derived for analyses of side-chain data for F16 and F65 are similar to the value (−2.9 kcal/mol) resolved from the quantitative EndoGluC footprinting studies of calcium-induced protection of E31 (Pedigo & Shea, 1995). The cooperativity determined for titrations of backbone resonances $D64_{C\alpha H}$ and $T26_{C\alpha H}$ was lower than that for Y138 in the C-terminal domain. Although the confidence intervals of ΔG_c for N-terminal domain resonances are broad, the values of ΔG_c segregate with the two affinity classes which would be consistent with the possibility that the phenylalanine residues monitor transitions distinct from those monitored by T26 and D64.

To explore the significance of these apparent differences and their dependence on experimental uncertainty, the experimental chemical shift data were perturbed with random error in the range of ±0.01 ppm and analyzed as described in Experimental Procedures. Average values resolved from analysis of three sets of *error-perturbed* chemical shift data

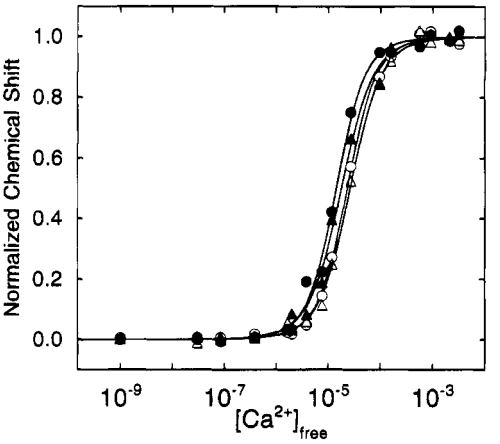

FIGURE 6: Calcium titration of calmodulin in 152 mM KCl buffer. Calcium-dependent changes in normalized chemical shift of resonances for $F16_{C\delta H}$ (●), $F65_{C\delta H}$ (▲), $T26_{C\alpha H}$ (○), and $D64_{C\alpha H}$ (△) *vs* the free calcium concentration (M) in each dialysate. Curves simulated with parameters resolved from best fits to model II (Table 2).

for $F16_{C\delta H}$, $T26_{C\alpha H}$, $D64_{C\alpha H}$, and $F65_{C\delta H}$ yielded parameters that were nearly identical to those reported for analysis of the experimental data (Table 3). The values of total free energy (ΔG_2) resolved for calcium-binding to calmodulin from the error-perturbed data differed by ≤0.07 kcal/mol from those reported in Table 2. The mean value of the cooperative free energies (ΔG_c) calculated from the error-perturbed data differed by ≤0.9 kcal/mol from those reported in Table 2. This supports the assertion that uncertainty in the chemical shift values (estimated at ≤0.01 ppm) does not significantly change resolved parameters or conclusions regarding the existence of two classes of isotherms for the N-terminal domain.

For the studies in 152 mM KCl, Figure 6 shows the isotherms resolved from the chemical shifts of $F16_{C\delta H}$, $T26_{C\alpha H}$, $D64_{C\alpha H}$, and $F65_{C\delta H}$ as a function of calcium concentration. As expected, the calcium binding affinity of calmodulin was less favorable in 152 mM KCl than in 92 mM KCl. For the four residues studied, these isotherms reflected the same relative order of median ligand activity (F16 < F65 < D64 < T26) as observed at lower KCl. However, the range between resolved total free energies was

narrower (0.72 kcal/mol) such that there were not two distinct classes of affinity or cooperativity (Table 2). The estimates of ΔG_c for calcium binding to sites I and II in the N-terminal domain are reported in Table 2. The parameters resolved from analysis of the corresponding *error-perturbed* chemical shift data are reported in Table 3.

With an increase in KCl, the ΔG_c for the backbone resonances of T26 and D64 did not change, whereas ΔG_c for the side-chain resonances of F16 and F65 was calculated to be less favorable (less negative). For the N-terminal domain, this lack of change or possible decrease in cooperativity with increasing salt concentration is in the direction opposite to that seen for isotherms resolved from the C-terminal domain probes and has not been reported previously for calcium binding. This behavior for the N-terminal domain of calmodulin contrasts with previous salt-dependent studies of calmodulin (Haiech *et al.*, 1981; Linse *et al.*, 1991) which reported that the value of ΔG_c for the N-terminal domain became more favorable (more negative) between 0 mM and 50 mM KCl. However, that study reported only (identical) lower limits of cooperativity at 100 and 150 mM KCl; thus, it is not possible to make a direct comparison with the values in Tables 2 and 3. Regardless of whether the data for F16 and F65 are interpreted as being in a cooperativity class distinct from that of T26 and D64, the isotherms do not indicate an increase in cooperativity with an increase in salt concentration and thus contrast with the salt-dependent behavior of Y138 in the C-terminal domain.

For the four residues of the N-terminal domain monitored in this study, it is not known to what degree their conformational response is linearly related to the occupancy of the nearest site. These resonances may be most sensitive to binding at site I or site II or may represent a weighted average of calcium binding to both sites in the N-terminal domain. Given that F16 and F65 are not directly involved in chelation of calcium and that their side chain protons are monitored by this NMR study, it is possible that the signal change of these residues contain contributions from global (interdomain) calcium-dependent changes of calmodulin. In the following discussion, we propose an alternative interpretation of the titration curves resolved for resonances of the N-terminal domain and consider several limiting cases.

Spectral Signal: Binding vs Conformational Change. In the NMR spectra of calmodulin, the change in position or intensity of a resonance as a function of calcium binding is the experimental signal monitored. The simple interpretation of change in that signal is that conformational changes have occurred in calmodulin in response to ligand binding; however, the extent of conformational change need not be linearly related to fractional occupancy of the nearest calcium-binding site. In fact, given the global conformational changes that are recognized to be induced by calcium binding locally, we might expect otherwise. Certainly in other allosteric systems, such as hemoglobin, the use of NMR to monitor a multitude of resonances has demonstrated unequivocally that the net quaternary response to ligand binding was composed of fractional and opposing changes distributed throughout the molecule (cf., Russu *et al.*, 1982). The challenge is to deconvolve the contributions from local binding and coupling to conformational change elsewhere in the molecule.

The two classes of isotherms observed at 92 mM KCl for the N-terminal domain residues (Figure 5) raise several issues pertinent to our interpretation of these isotherms. They include (a) the difference between calcium-dependent responses of backbone and side-chain resonances (i.e., $D64_{C\alpha H}$ *vs* $F65_{C\delta H}$), (b) the equivalent response of the β-sheet resonances in site I ($T26_{C\alpha H}$) and site II ($D64_{C\alpha H}$), and (c) the differences between their salt-dependent changes (i.e., their response to a solution perturbation). They illustrate the complexity of relating binding to conformational change and distinguishing heterogeneity and cooperativity in the binding process.

The data are of sufficient quality to contradict the assumption that all four resonances represent the average binding properties of the N-terminal domain. An intuitively attractive explanation for two classes of isotherms observed for spectral change in a domain is that each residue reports the fractional occupancy of only that site of which it is a member (as defined by the primary sequence; see Figure 1). Such individual-site fractional saturation would be described by the equations below (Ackers *et al.*, 1983), where sites "a" and "b" do not necessarily correlate with sites I and II and site "a" is defined to be the higher affinity site.

$$\bar{Y}_a = \frac{k_1[X] + k_1k_2k_{12}[X]^2}{(1 + (k_1 + k_2)[X] + k_1k_2k_{12}[X]^2)} \quad (7)$$

$$\bar{Y}_b = \frac{k_2[X] + k_1k_2k_{12}[X]^2}{(1 + (k_1 + k_2)[X] + k_1k_2k_{12}[X]^2)} \quad (8)$$

However, a consequence of this interpretation would be that the titration curves for the backbone $D64_{C\alpha H}$ and side-chain $F65_{C\delta H}$ protons (residues both in site II) should be equivalent. Their separation contradicts this or challenges the definition of a site.

There are several other interpretations. It is possible that the resolved transitions do not represent true thermodynamic binding isotherms but instead the normalized signal is a manifestation of unequal fractional contributions (f_i) from two individual-site isotherms (i.e., Signal $= f_a\bar{Y}_a + f_b\bar{Y}_b$ where $f_a \neq f_b$). However, there is no way to obtain an independent determination of the coefficients in this expression from these data. This is the same difficulty faced by assuming that the signal for the pair of resonances (F16 and F65) monitoring apparently higher affinity binding may be influenced by calcium binding to sites III and IV (i.e., Signal $= f_a\bar{Y}_a + f_b\bar{Y}_b + f_c\bar{Y}_c + f_d\bar{Y}_d$). This cannot be addressed directly because of the paucity of probes in the C-terminal domain. A simpler interpretation is as follows.

On the basis of these NMR titrations and other data (cf., Crouch & Klee, 1980; Linse *et al.*, 1991; Kilhoffer *et al.*, 1992), it is evident that the binding of calcium to sites I and II is not independent and that the intrinsic affinities are not identical. However, as has been shown for other macromolecular systems (Ackers *et al.*, 1983; Senear & Brenowitz, 1991) as well as calmodulin (Wang, 1985; Haiech *et al.*, 1981), there are many combinations of microscopic equilibrium constants that may give equivalent macroscopic binding behavior. The purpose of the following section is to explore combinations of microscopic equilibrium constants that are consistent with these data.

We make the assumptions that (a) the signal changes at N-terminal residues F16, T26, D64, and F65 are affected by

calcium binding at sites I and II only, and (b) sites I and II may be heterogeneous and cooperative. In view of the separation of the curves but their evident positive cooperativity, we propose that the binding curve for $D64_{C\alpha H}$ represents the total fractional saturation of the domain ($\bar{Y}_t$), which may be formulated as the average of the individual-site equations.

$$\bar{Y}_t(X) = (\bar{Y}_a + \bar{Y}_b)/2 \quad (9)$$

(This is equivalent to $\bar{Y}_I$ (eq 2) for two equal, independent sites or $\bar{Y}_{II}$ (eq 3) for two possibly heterogeneous, cooperative sites.) By extension, this formulation implies that the $T26_{C\alpha H}$ resonance is described by eq 9 as well.

The experimental finding that D64 and T26 respond in tandem in these equilibrium studies is supported by several independent lines of evidence for congruent changes in the β sheet regions of sites I and II. Stoichiometric NMR studies showed that T26 and D64 in wild type calmodulin tracked together and changed in response to the second pair of calcium ions binding (Klevit *et al.*, 1984; Starovasnik *et al.*, 1992). Fluorescence studies of tryptophan-substituted mutants of calmodulin (Kilhoffer *et al.*, 1992) showed that the conformations of both T26W (in site I) and T62W (in site II) responded to binding of both the third and fourth ligands onto calmodulin, reporting on the average properties of the N-terminal domain. NMR studies of peptides representing EF-hands of troponin C have shown that calcium binding to one site in an EF-hand pair may induce dimerization and conformational change in the opposing site, preceding binding in that site (Shaw *et al.*, 1991). Thus, it seems justified to propose that the binding curve for $D64_{C\alpha H}$ represents the total fractional saturation of the domain ($\bar{Y}_t$). Therefore, because F65 (and F16) appears to reflect a higher affinity transition than does D64 (and T26), we propose that $F65_{C\delta H}$ represents fractional occupancy of the N-terminal domain site with higher intrinsic affinity for calcium ($\bar{Y}_a$; eq 7). (From the NMR data alone, it is not possible to assign site "a" to correspond to a particular site (i.e., I or II).)

By interpreting the isotherm for $F65_{C\delta H}$ as representing $\bar{Y}_a$ (eq 7), and the binding curve for $D64_{C\alpha H}$ to $\bar{Y}_t$ (eq 9), we can explore the sets of equilibrium constants that are consistent with both sets of data. These may provide insight into the possible range of heterogeneity and cooperativity between sites. If the value of microscopic cooperativity (k_{12}) is held constant, it is possible to use NONLIN to solve simultaneously for the values of the intrinsic equilibrium constants (k_1, k_2) that minimize the variance for both data sets simultaneously. Several of these analyses are presented in Table 4 and shown in Figure 7. Corresponding calculated (not resolved) values of the macroscopic free energies (ΔG_1 and ΔG_2) and their propagated confidence intervals are given for comparison to the values resolved from experimental studies (in Tables 2 and 3).

While it is straightforward to determine that the system must be cooperative by at least 1 kcal/mol, it is impossible to determine a unique value for Δg_{12} because there is a high degree of compensation between cooperativity and heterogeneity. The partitioning of cooperative free energy between unequal sites favors the weaker site (Ackers *et al.*, 1983). This effect can be seen by inspection of parameters in Table 4. As the cooperativity changes from −3 to 0 kcal/mol, Δg_1 changes by 0.6 kcal/mol, whereas Δg_2 changes by 2.2 kcal/mol; as expected, the weaker site is affected most by the change in cooperative free energy. Almost complete compensation is observed between cooperativity and the affinity of the weaker site, such that there is very little difference in the values of $\bar{Y}_t$ for significantly different values of Δg_{12}

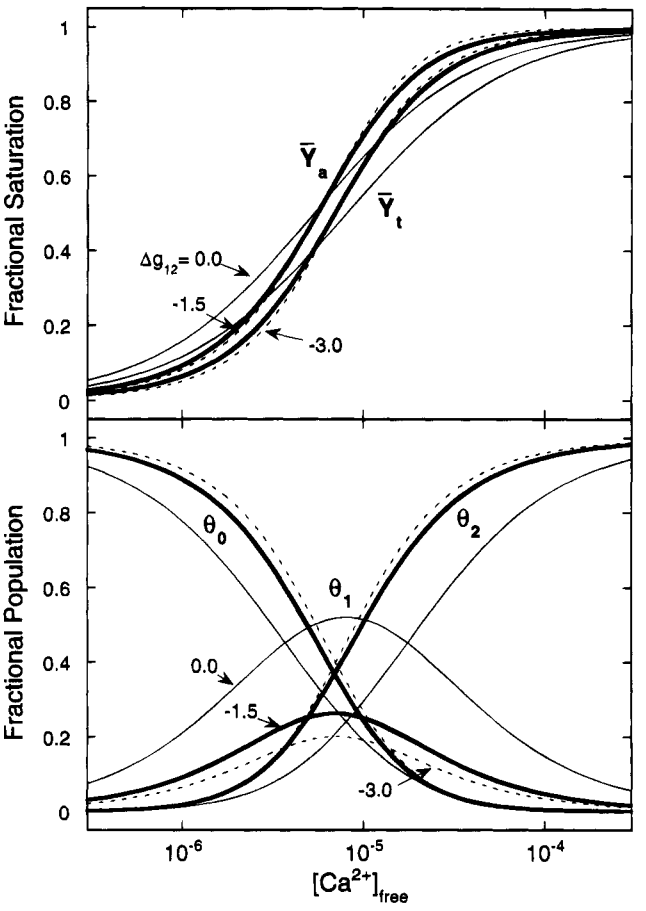

FIGURE 7: Effect of variable cooperativity on simulated calcium titrations of calmodulin in 92 mM KCl. Curves simulated using $\Delta g_{12} = 0$ (thin solid curve), −1.5 (thick solid curve), and −3 kcal/mol (dashed curve) and corresponding values from Table 4. (a) Simulation of normalized chemical shift of the resonances for $F65_{C\delta H}$ as $\bar{Y}_a$ (eq 7) and $D64_{C\alpha H}$ as $\bar{Y}_t$ (eq 9). (b) Corresponding calculation of fractional abundance of apo (θ_0), singly-ligated (θ_1), and doubly-ligated (θ_2) N-terminal domain sites.

Table 4: Simultaneous Analysis[a] of $D64_{C\alpha H}$ as $\bar{Y}_t$ and $F65_{C\delta H}$ as $\bar{Y}_a$ in the Calcium Titration of Calmodulin at 92 mM KCl[b]

Δg_{12}[c]	Δg_1	Δg_2	$\sqrt{\text{var}}$[d]	ΔG_1[e]	ΔG_2
0.0	−7.12 ± 0.10	−6.63 ± 0.43	0.0178	−7.33 ± 0.16	−13.76 ± 0.43
−0.5	−6.94 ± 0.09	−6.42 ± 0.33	0.0143	−7.14 ± 0.09	−13.86 ± 0.26
−1.5	−6.67 ± 0.19	−5.78 ± 0.37	0.0110	−6.77 ± 0.10	−13.93 ± 0.18
−3.0	−6.54 ± 0.23	−4.37 ± 0.36	0.0103	−6.55 ± 0.20	−13.91 ± 0.13

[a] Fitting $D64_{C\alpha H}$ as $\bar{Y}_t$, average fractional saturation of the domain, and $F65_{C\delta H}$ as $\bar{Y}_a$, the fractional occupancy of the site with higher intrinsic affinity. [b] Data spanned free calcium from 1 nM to 1.1 mM (pCa = 9.0−2.97). [c] All Gibbs free energies are expressed in kcal/mol (1 kcal = 4.184 J); lowercase g is used to emphasize that these represent microscopic free energies (eqs 6 and 7). Value of Δg_{12} ($-RT \ln k_{12}$) was fixed to value given; Δg_1 ($-RT \ln k_1$) and Δg_2 ($-RT \ln k_2$) are fitted values resolved from analysis of $D64_{C\alpha H}$ as $\bar{Y}_t$ and $F65_{C\delta H}$ as $\bar{Y}_a$. To overestimate the uncertainty, the greater of the positive or negative limit of each asymmetric 65% confidence interval was tabulated. [d] Correlation coefficients, magnitude, and distribution of residuals also were evaluated but not shown. [e] Values for ΔG_1 and ΔG_2 were calculated from resolved values for Δg_1 and Δg_2 ($K_1 = k_1 + k_2$ and $K_2 = k_1 k_2 k_{12}$); errors on ΔG_1 and ΔG_2 were propagated by NONLIN.

(−1.5 *vs* −3 kcal/mol; see Figure 7a; compare dashed and dark solid curves.). The same is true for Y_a. In addition, the calculated values of ΔG_2 (total free energy; Table 4) are similar in spite of very different partitioning of the total energy between intrinsic binding and cooperativity. Figure 7b shows that in spite of this high degree of compensation, there would be an advantage to resolving individual ligation species of wild-type protein (see θ_0, θ_1, and θ_2 in Figure 7b). Although there is very little difference in the populations of apo (θ_0) and doubly liganded species (θ_2) for a difference of −1.5 kcal/mol in cooperativity (a factor of 13 difference in k_{12}), there would be a difference of >6% in the population of singly liganded species (θ_1).

It is clear from this attempt to deduce intrinsic and cooperative equilibrium constants from the N-terminal domain binding data that more information is required to define these parameters completely. However, given the constraints of the proposed model, it appears that the higher affinity N-terminal domain site has an intrinsic affinity of approximately −7 kcal/mol. The intrinsic affinity of the lower affinity site cannot be estimated without knowledge of the partitioning of free energy between cooperativity and heterogeneity.

While the differences between resolved affinity and cooperativity for D64 and F65 are perplexing because they are nearest neighbors in a calcium-binding site, these differences may be revealing complexities of the functional energetics of calmodulin (as well as illustrating the difficulty of inferring a relationship between a spectroscopic signal and the binding events that are driving the conformational change). It is important to recognize that in calcium-saturated calmodulin, the distance between these protons ($D64_{C\alpha H}$ and $F65_{C\delta H}$) is greater than 6 Å. The NMR data demonstrate that they respond slightly differently to calcium binding, possibly providing new clues to conformational coupling in calmodulin. A combination of experimental techniques will be required to determine the origins of this coupling, so that we will better understand the microscopic switching behavior of this regulatory protein.

Differences in the Salt-Dependent Behavior of the Domains. These analyses (Figure 7 and Table 4) make clear that four signals are insufficient to determine the degree to which significant heterogeneity may be masked by cooperativity in the N-terminal domain of calmodulin. One way to probe these chemical properties is to perturb the system through changes in solution conditions. For resonances at 92 mM KCl, the difference between resolved values of total free energy (1.17 kcal) was more pronounced than the difference (0.72 kcal) for the titration at 152 mM KCl. One interpretation is that heterogeneity between sites "a" and "b" was reduced by the increase in KCl (i.e., the affinities of both sites "a" and "b" decreased at higher concentrations of KCl, but site "a" experienced a larger decrease in affinity than did site "b"). This difference in the salt-dependency of affinity at sites "a" and "b" might occur because of specific differences in the charged residues in sites I and II or in other regions of the α and β segments (see Figure 1). An alternative explanation is that the heterogeneity has not changed, but there has been a change in the intradomain cooperativity. Inspection of eq 6 shows that K_c increases if k_h decreases and k_{12} is unchanged. Thus, if there were a decrease in the apparent heterogeneity between the sites, then the intradomain cooperativity (k_{12}) also must have decreased for a case in which the resolved value of K_c did not change (e.g., the similar values for T26 and D64). Another interpretation of the salt-dependent differences in values of ΔG_c calculated for resonances in the N-terminal domain would be that KCl diminishes otherwise favorable interdomain interactions that preferentially affect F16 and F65, possibly screening interactions that might be critical to a calcium-induced switching process (Pascual-Ahuir *et al.*, 1991).

It is noteworthy that an increase in salt induced an increase in apparent cooperativity of the sites in the C-terminal domain, in contrast to the behavior of the N-terminal domain. The increase in cooperativity that was resolved from analysis of the fluorescence data is consistent with either (a) a decrease in heterogeneity (i.e., greater similarity of k_1 and k_2) or (b) an increase in microscopic cooperativity (k_{12}) for calcium binding to sites III and IV in the C-terminal domain. However, from analysis of a single isotherm for the domain, it is not possible to determine directly the relative contributions of these changes. At the least, the effects of salt on calcium binding to the C-terminal domain are evidently different from its effects on the N-terminal domain. This would be consistent with studies of mutations of the third position (+Y) in sites II and III that lead to opposite effects on cooperativity (Waltersson *et al.*, 1993). Theoretical simulations of the counterion distribution showed a strong dependence on the calcium occupancy of sites and larger differences between sites III and IV than between sites I and II (Svensson *et al.*, 1993).

Interdomain Cooperativity. Several studies have reported that a subset of residues in the N-terminal domain respond to C-terminal binding by exhibiting biphasic behavior. In the 1-D NMR experiments of this report, biphasic behavior might have been manifest as a mixture of fast exchange (C-terminal domain binding) and slow exchange (N-terminal domain binding) behavior. Alternatively, biphasic behavior might have been observed as a nonmonotonic change in the chemical shift of a resonance over the course of a calcium titration. Both have been reported for N-terminal resonances. Klevit *et al.* (1984) noted that several N-terminal methionine resonances were in a class that exhibited slow exchange behavior as the C-terminal domain bound calcium and fast exchange behavior as the N-terminal domain sites bound calcium. Starovasnik *et al.* (1992) reported nonmonotonic changes in the chemical shift for $T26_{C\alpha H}$ for binding-site mutants of calmodulin. Neither of these types of biphasic response was observed for the resonances of wild-type calmodulin monitored in this study.

There were strong indications of interdomain interactions found in the quantitative proteolytic footprinting studies (Pedigo & Shea, 1995; Verhoeven & Shea, 1993; Shea, 1992). Several residues (E31, R37, and S38) in the helix leading out of site I in the N-terminal domain responded to C-terminal binding events by exhibiting biphasic susceptibility to proteolysis. However, the NMR studies reported here did not monitor any residue in the sequence between sites I and II; thus, it is not possible to make a direct comparison.

Consistency of Macroscopic Free Energies. The binding parameters resolved from these discontinuous equilibrium titrations of calmodulin monitored by NMR may be compared to those resolved by other methods for determining microscopic and macroscopic equilibrium constants. The dialysates of calmodulin used to define the titration at 92

mM KCl have also been studied in this laboratory using quantitative proteolytic footprinting methods and serve as a test of external consistency. For binding of calcium to the N-terminal domain, the values of ΔG_2 reported in Table 2 agree well with the values resolved from the induced protection phase of the biphasic susceptibility profile for R37 as probed with thrombin (Verhoeven & Shea, 1993). The values resolved from analysis of the NMR-derived isotherm for F16 are similar to, but slightly lower affinity than those resolved for the induced protection phase of the biphasic susceptibility profile for the EndoGluC probe at E31 (Pedigo & Shea, 1995). For the C-terminal domain, the value of ΔG_2 in Table 1 agreed well with −15.95 kcal/mol resolved from the calcium-induced protection of R106 as probed with thrombin (Verhoeven & Shea, 1993). Preliminary studies of quantitative proteolytic footprinting of titrations of calmodulin indicate that F65 has a monotonic susceptibility to proteolysis by chymotrypsin (data not shown), which is consistent with these NMR studies. It is not possible to compare the NMR studies of the N-terminal domain with results from an optical spectroscopic method because of the lack of reporter groups in that domain. However, as shown in Figure 4, there was excellent agreement between the best-fit curves corresponding to the NMR and tyrosine fluorescence studies of Y138 in the C-terminal domain.

The free energies of calcium binding obtained from this discontinuous equilibrium NMR method may be corroborated by comparison with macroscopic equilibrium constants. The total free energy of binding four calcium ions to calmodulin at 92 mM KCl may be estimated from the NMR data by summing the average free energy determined for the N-terminal domain (e.g., average of T26 and D64 = −13.5 kcal/mol) and a value for the single probe of the C-terminal domain (e.g. Y138 = −16.1 kcal/mol). This yields an estimate of −29.6 kcal/mol for the total free energy which is in excellent agreement with −28.5 kcal/mol reported by Crouch and Klee (1980) and −29 kcal/mol reported by Linse *et al.* (1991) for studies under similar conditions of salt, pH, and temperature.

SUMMARY

We have reported the first resolution of equilibrium calcium-binding isotherms of calmodulin using NMR spectroscopy. This study builds on pioneering stoichiometric binding studies of calmodulin monitored by NMR (Klevit *et al.*, 1984; Seamon, 1980), but allows estimates of free energies of binding and cooperativity. This study depended critically on the use of a discontinuous titration approach (Pedigo & Shea, 1995) to establish equilibrium at the high protein concentrations required for an NMR experiment. We found that both of the domains exhibited positive cooperativity of more than 1 kcal/mol in binding calcium, and that with an increase in KCl the cooperativity increased for the C-terminal domain, but was unchanged or decreased for residues in the N-terminal domain. In the N-terminal domain, there were two classes of response separated by ~1 kcal/mol, suggesting differences between the intrinsic affinities of calcium for sites I and II.

These are the first spectroscopic experiments to resolve the energetics of calcium binding to the N-terminal domain of wild-type calmodulin and complement quantitative proteolytic footprinting studies (Pedigo & Shea, 1995; Verhoeven & Shea, 1993). These two experimental approaches have different advantages and sources of systematic errors (e.g., drying and reconstitution of dialysates for NMR studies *vs* enzymatic digestion). However, there is excellent agreement between these techniques for quantitatively monitoring residue-specific conformational change that occurs upon calcium binding. There is similar agreement between titrations monitored by calcium-dependent changes in the fluorescence intensity and the NMR resonance area for $Y138_{C\delta H}$. Results from these studies also compare favorably to those from macroscopic binding studies (Crouch & Klee, 1980; Linse *et al.*, 1991; Haiech *et al.*, 1981) and are consistent with the model of Kilhoffer *et al.* (1992).

Calmodulin is finely tuned to balance the demands of metal binding and molecular recognition of protein targets. The interplay between the heterogeneous and cooperative nature of calcium binding makes the dissection of microscopic binding equilibria in this system very challenging. More advanced NMR methods and orthogonal techniques will be required to resolve substantive issues raised here regarding the differences between the response of backbone protons (e.g., T26 and D64) and side-chain protons (e.g., F16 and F65) within the same site or domain. The salt dependence of calcium binding explored in this study is one of many variables that must be explored to deconvolve the molecular origins for coupling between site occupancy and conformational change. The ultimate determination of intrinsic free energies for the four calcium-binding sites and the nature and degree of intra- and interdomain cooperativity will require the application of many such perturbations studied by NMR and other methods that can monitor residue-specific responses at multiple positions simultaneously.

ACKNOWLEDGMENT

We would like to thank William R. Kearney, Director of the Univ. of Iowa College of Medicine NMR Facility, for assistance with these studies; R. Mauer and P. Howard, Univ. of Oregon, for the overexpression vector used for calmodulin; the Univ. of Iowa College of Medicine Protein Structure Facility for the use of the SLM 4800 Fluorimeter; and the Univ. of Iowa Diabetes and Endocrinology Center Molecular Biology facility for DNA sequencing. We would like to thank Charles A. Swenson, Andrew D. Robertson and the reviewers for critical comments on the manuscript.

REFERENCES

Ackers, G. K., Shea, M. A., & Smith, F. R. (1983) *J. Mol. Biol. 170*, 223−242.
Akke, M., Forsén, S., & Chazin, W. J. (1991) *J. Mol. Biol. 220*, 173−189.
Aulabaugh, A., Niemczura, W. P., & Gibbons, W. A. (1984) *Biochem. Biophys. Res. Commun. 118*, 225−232.
Babu, Y. S., Bugg, C. E., & Cook, W. J. (1988) *J. Mol. Biol. 204*, 191−204.
Bayley, P. M., Ahlstrom, P., Martin, S. R., & Forsén, S. (1984) *Biochem. Biophys. Res. Commun. 120(1)*, 185−191.
Bayley, P. M., & Martin, S. R. (1992) *Biochim. Biophys. Acta Protein Struct. Mol. Enzymol. 1160*, 16−21.
Brenowitz, M., Senear, D. F., Shea, M. A., & Ackers, G. K. (1986) *Methods Enzymol. 130*, 132−181.
Cohen, P., & Klee, C. B. (Eds.) (1988) *Calmodulin*, Elsevier, New York.
Crouch, T. H., & Klee, C. B. (1980) *Biochemistry 19*, 3692−3698.
Dalgarno, D. C., Klevit, R. E., Levine, B. A., Williams, R. J. P., Dobrowolski, Z., & Drabikowski, W. (1984) *Eur. J. Biochem. 138*, 281−289.

Evans, J. S., Levine, B. A., Williams, R. J. P., & Wormald, M. R. (1988) in *Calmodulin* (Cohen, P., & Klee, C. B., Eds.), pp 57−82, Elsevier, New York.
Haiech, J., Klee, C. B., & Demaille, J. G. (1981) *Biochemistry 20*, 3890−3897.
Hoffman, R. C., & Klevit, R. E. (1991) *Tech. Protein Chem. II*, 383−391.
Ikura, M. (1986) *Biochim. Biophys. Acta 872*, 195−200.
Ikura, M., Barbato, G., Klee, C. B., & Bax, A. (1992a) *Cell Calcium 13*, 391−400.
Ikura, M., Clore, G. M., Gronenborn, A. M., Zhu, G., Klee, C. B., & Bax, A. (1992b) *Science 256*, 632−638.
Ikura, M., Hiraoki, T., Hikichi, K., Mikuni, T., Yazawa, M., & Koichi, Y. (1983a) *Biochemistry 22*, 2568−2572.
Ikura, M., Hiraoki, T., Hikichi, K., Mikuni, T., Yazawa, M., & Yagi, K. (1983b) *Biochemistry 22*, 2573−2579.
Ikura, M., Hiraoki, T., Hikichi, K., Minowa, O., Yamaguchi, H., Yazawa, M., & Yagi, K. (1984) *Biochemistry 23*, 3124−3128.
Ikura, M., Minowa, O., & Hikichi, K. (1985) *Biochemistry 24*, 4264−4269.
Johnson, M. L., & Frasier, S. G. (1985) *Methods Enzymol. 117*, 301−342.
Kilhoffer, M.-C., Kubina, M., Travers, F., & Haiech, J. (1992) *Biochemistry 31*, 8098−8106.
Klevit, R. E. (1983) *Methods Enzymol. 102*, 82−104.
Klevit, R. E., Dalgarno, D. C., Levine, B. A., & Williams, R. J. P. (1984) *Eur. J. Biochem. 139*, 109−114.
Kraulis, P. J. (1991) *J. Appl. Crystallogr. 24*, 946−950.
Kretsinger, R. H. (1976) *Annu. Rev. Biochem 45*, 239−265.
Linse, S., Helmersson, A., & Forsen, S. (1991) *J. Biol. Chem. 266*, 8050−8054.
Martin, S. R., Andersson-Teleman, A., Bayley, P. M., Drakenberg, T., & Forsén, S. (1985) *Eur. J. Biochem. 151*, 543−550.
Meador, W. E., Means, A. R., & Quiocho, F. A. (1992) *Science 257*, 1251−1255.
Meador, W. E., Means, A. R., & Quiocho, F. A. (1993) *Science 262*, 1718−1721.
Pascual-Ahuir, J.-L., Mehler, E. L., & Weinstein, H. (1991) *Mol. Eng. 1*, 231−247.
Pedigo, S., & Shea, M. A. (1995) *Biochemistry 34*, 1179−1196.
Putkey, J. A., Slaughter, G. R., & Means, A. R. (1985) *J. Biol. Chem. 260(8)*, 4704−4712.
Ross, J. B. A., Laws, W. R., Rousslang, K. W., & Wyssbrod, H. R. (1992) in *Topics in Fluorescence Spectroscopy, Volume 3: Biochemical Applications* (Lakowicz, J. R., Ed.), pp 1−63, Plenum Press, New York.
Russu, I. M., Ho, N. T., & Ho, C. (1982) *Biochemistry 21*, 5031−5043.
Seamon, K. B. (1980) *Biochemistry 19*, 207−215.
Seeholzer, S. H., & Wand, A. J. (1989) *Biochemistry 28*, 4011−4020.
Senear, D. F., & Brenowitz, M. (1991) *J. Biol. Chem. 266*, 13661−13671.
Shaw, G. S., Golden, L. F., Hodges, R. S., & Sykes, B. D. (1991) *J. Am. Chem. Soc. 113*, 5557−5563.
Shea, M. A. (1992) *Biophys. J. 61(2, part 2)*, A413 (Abstract).
Starovasnik, M. A., Su, D-A., Beckingham, K., & Klevit, R. E. (1992) *Protein Sci. 1*, 245−253.
Svensson, B., Jönsson, B., Thulin, E., & Woodward, C. E. (1993) *Biochemistry 32*, 2828−2834.
Tabor, S., & Richardson, C. C. (1985) *Proc. Natl. Acad. Sci. U.S.A. 262*, 1074−1078.
Teleman, A., Drakenberg, T., & Forsén, S. (1986) *Biochim. Biophys. Acta 873*, 204−213.
Tsai, M.-D., Drakenberg, T., Thulin, E., & Forsen, S. (1987) *Biochemistry 26*, 3635−3643.
Török, K., & Whitaker, M. (1994) *BioEssays 16(4)*, 221−224.
Török, K., Lane, A. N., Martin, S. R., Janot, J.-M., & Bayley, P. M. (1992) *Biochemistry 31*, 3452−3462.
Urbauer, J. L., Short, J. L., Dow, L. K., & Wand, A. J. (1995) *Biochemistry 34*, 8099−8109.
Verhoeven, A. S., & Shea, M. A. (1993) *Biophys. J. 64*, A169.
Waltersson, Y., Linse, S., Brodin, P., & Grundström, T. (1993) *Biochemistry 32*, 7866−7871.
Wang, C.-L. A. (1985) *Biochem. Biophys. Res. Commun. 130(1)*, 426−430.
Wang, C.-L. A., Leavis, P. C., & Gergely, J. (1984) *Biochemistry 23*, 6410−6415.
Wishart, D. S., Sykes, B. D., & Richards, F. M. (1991) *J. Mol. Biol. 222*, 311−333.

BI950158+